

## CHAPTER 191

### A MODELING SYSTEM FOR COASTAL OIL SPILL RISK ANALYSIS

Shiao-Kung Liu and Jan J. Leendertse

#### INTRODUCTION

At present, the Prudhoe Bay oil field in Alaska contributes a substantial amount of the domestic oil production of the United States. Oil is also expected to be present on the continental shelf of Alaska, and it is estimated that approximately 28 percent of the total U. S. reserve is located beneath the shallow ice covered seas of the Alaskan continental shelf. To explore and to exploit these oil rich resources, engineers are confronted with hostile oceanographic conditions such as high tides, waves, strong currents and sea ice. The same area is also rich in fishery resources. Being one of the most productive fishing grounds in the northern Pacific, the potential ecological impact due to an oil spill is of a major concern. This paper describes the methodologies used for the development of a modeling system for the oil risk analysis. The system is designed with generality in mind so it can be used for other coastal areas.

The development of three dimensional models used in the modeling system described here have been published in the earlier International Coastal Engineering Conferences (Liu and Leendertse, 1982, 1984, 1986) and a report published recently by RAND (Liu and Leendertse, 1987). In the oil-spill risk analysis, these three dimensional hydrodynamic models are coupled to a two-dimensional stochastic weather model and an oil weathering model.

Before decisions are made concerning which specific offshore areas to lease for exploration or exploitation, the responsible government agency must balance orderly resources development against the protection of human, marine, and coastal environment, to ensure that the public receives a fair return for these resources. In studies made for this purpose, the impact of hypothetical oil spill are considered. Not only are oil spill pathways required for the impact analysis, in certain instances knowledge about the extent of oil spill is required as well as about the oil concentration that would occur in the water column. This paper presents an efficient way for making the risk analysis while maintaining the essential dynamics of the processes involved.

## THE MODELING APPROACH FOR LONG DURATION WIND DRIVEN CURRENTS

As the three-dimensional models made of the different offshore areas of Alaska simulate the movements of water, and as a model is available to simulate wind sequences offshore, it would be logical to use these models in the computation of oil spill movements. To use these models effectively, we have developed a method to compute wind driven currents. This method retains the dynamic detail of the three-dimensional model and yet is approximately two orders of magnitude more efficient than the simulations with the three-dimensional model; it is called the "wind-driven response function method." In essence, the method extends the basic idea of the "drift ratio" between the wind speed and current speed except that the ratio changes in time and over space and is derived from the three-dimensional model.

The traditional, simple fixed drift-ratio method has many difficulties when applied in the Alaskan coastal waters. It is applicable only for cases of steady wind with constant speed blowing over water with finite depth and with no boundaries. However, the concept of the "drift ratio" is a good one—but we need to include more dynamics in it.

In examining the fundamental dynamics of wind-driven currents, even under the assumption of steady (in time), constant (over space) wind and an infinitely long straight coastline, wind-driven currents over water of finite depth do vary both in direction and speed at the surface and at different levels to satisfy the law of conservation of mass. Using information on the distance from shore, wind direction, and local depth, Ekman (1905) worked out the variabilities of drift currents by using highly simplified terms in the equations of motion. On the other hand, to include more terms would require the solution of the complete three-dimensional model.

In our study, time-varying response functions under various wind conditions were developed using wind stress associated with the marine wind speed. Reverse procedures (convolution) were then used during the oil trajectory simulation; therefore, they are not linear with respect to local wind speed. Since the response functions for all layers are derived from the three-dimensional model, time-varying effects (such as a moving storm, deepening of a mixed layer, and inertia components) are included in the oil spill trajectory computation. The method is very efficient, however, the oil spill trajectory model was programmed so that the drift ratio and deflection angle from field observations under various conditions over an entire area can, as an option, still be used for the computation of oil movement.

Wind driven currents over stratified waters vary with the degree of vertical stability associated with the stratification. To illustrate this point we use a simple case where the time series of water movement at two nearby locations in Norton Sound is plotted (Fig. 1), and wind from the east is applied for a duration of 12 hours (close to the inertial period) over the water. The response of surface water at two nearby locations is not the same to satisfy the continuity principle of water within a bay. Response functions over the water column of the entire modeled area are calculated by the three-dimensional model.

To generate the complete set of response functions, five computer simulation runs are needed. One computer run is without wind but with tide. The other four computer runs are with tides and with wind from each of four directions. The four response functions set are derived from the difference between them and the one with tide as the only forcing function. The level of tidal currents at different areas produces variable wind responses under the same wind, so the tide has to be included when deriving wind response functions, otherwise they will be overestimated. This is why in a coastal area with strong tidal currents the drift ratio would be lower than in the open ocean because of the quadratic nature of the bottom friction.

When response functions are saved in discrete time intervals (30 minutes was used) the drift velocity at a certain time is computed by numerical convolution.

$$U_{ij}(n \Delta t) = \Delta t \sum_{k=0}^n (W^2) h_{ij}(n \Delta t - k \Delta t) \quad (1)$$

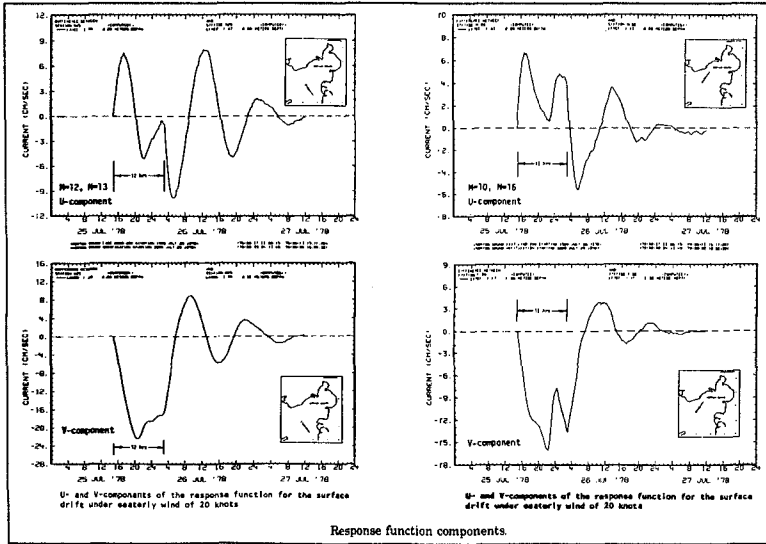


Fig 1

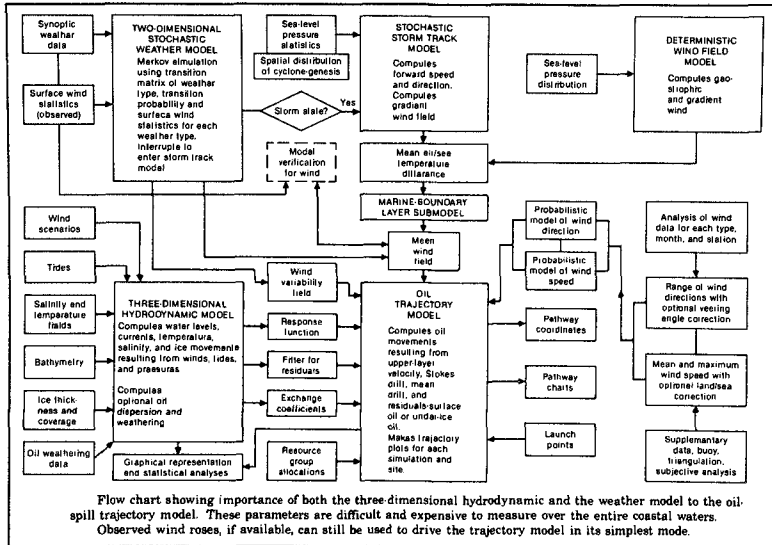


Fig 2

where  $W$  = wind speed from a certain direction,

$U_{ijk}$  = velocity at a particular point ( $i, j, k$ ), and

$h_{ijk}$  = time domain response function between squared wind speed and velocity at point ( $k, j, k$ ).

With this formula the velocity at point  $i, j, k$  can be determined if the wind speed from a specific direction is known, as well as the response function.

The same principle applies for complex wind scenarios, then the vectorial decomposition is involved.

### COMPUTING OIL BEHAVIOR UNDER ICE

In the absence of a current, oil released in a water column will rise and be trapped underneath the ice. Under porous young ice during formation, oil will initially undergo a certain degree of vertical migration through the vertical brine channels. Most oil is initially in the form of droplets until a lateral slick is formed. The oil sheet tends to spread with an obtuse contact angle. For typical Alaska Prudhoe Bay crude oil, the average observed values of interfacial surface tension, density, and the contact angle are 31 dynes/cm, 0.911 g/cc, and 20°, respectively (Kovacs et al., 1980). The static thickness of the same oil is approximately 1.2 cm. Since the dynamic pressure exerted by a moving current on an oil slick of finite length tends to balance between the front and the back faces, the equilibrium thickness should be the same for both unaccelerated and static slicks.

The bottom roughness of ice not only determines the amount of oil that may be trapped beneath it, it also influences the speed of oil movement under moving currents. Using a radar echo sounding system, Cox et al. (1980) made extensive measurements of ice bottom morphology and found the standard variation of ice thickness to be 3.1 cm over a mean thickness of 1.53 m in an undeformed shore-fast ice zone near Prudhoe Bay. The thickness of ice was also found to be inversely proportional to the thickness of snow cover over it. The snow acts as an insulator that reduces heat exchange from the sea water through the ice to the atmosphere and thus retards the growth rate. Consequently, a substantial quantity of oil can be retained underneath the pack ice. Under weak currents, trapped oil will travel with the pack ice. The movement of oil under this condition would be identical to the computed movement of ice described above but the shear stress coefficients between water and ice are reduced.

Under strong "relative currents" (between water and ice), oil will travel at a speed different from the ice and currents. To compute the movement of oil under these conditions, in the three-dimensional model we adapted a method developed by Cox et al. (1980) with parameters evaluated from laboratory tests. This method involves the evaluation of a critical relative velocity between ice and water. Using  $\rho_w$  to represent the density of sea water in the surface layer of our computation, the critical velocity for the incipient motion with large roughness is approximately:

$$u_{\text{critical}} = 1.5 \left[ \frac{\rho_o + \rho_w}{\rho_o \rho_w} \right] \left[ \sigma_{o/w} g (\rho_w - \rho_o) \right]^{1/4} \quad (2)$$

in which  $\rho_o$ ,  $\sigma_{o/w}$  are, respectively, the density of oil and the surface tension at the oil/water interface. With the aforementioned typical values observed in the Beaufort Sea, this critical value is approximately 21 cm/sec.

Equation (2) is developed considering the formation of Kelvin-Helmholtz type instability, which exerts a limit on the thickness of an oil slick near the head region. A multiplier of 1.5 on the right-hand side of Eq. (2) was used considering the actual velocity that would cause droplet tearing. Ultimate slick failure occurs at about twice the critical velocity.

According to Cox et al. (1980), the critical velocity at which oil begins to move relative to the water when the relative velocity between ice and water is:

$$u_{oil} = u_{water} \left[ 1 - \left( \frac{\kappa}{A F_{\delta}^2 + B} \right)^{1/2} \right] \quad (3)$$

where  $\kappa$  is the amplification factor and  $F_{\delta}$  is a slick densimetric Froude number defined by:

$$F_{\delta} = \frac{u_{water}}{\sqrt{[(\rho_w - \rho_o)/\rho_w] g \delta}} \quad (4)$$

in which  $\delta$  represents the equilibrium slick thickness.

Equation (3) is derived from the momentum balance between form drag, oil/water interfacial shear stress, and the retarding of oil/ice frictional force. Constants  $A$  and  $B$  in the equation contain the effects of frontal shear and plane shear, as well as the normal force from oil's buoyance against the ice. For the field conditions of the model areas, the values of these coefficients are 1.75 and 0.115. The amplification factor  $\kappa$  equals unity for a hydrodynamic smooth region and is greater than zero for rough surfaces. For the field conditions in the model areas, the factor was given a value of 1.105. To determine the equilibrium oil slick thickness from the density of the oil, we used an empirical relation. The empirical difference is:

$$\delta = 1.67 - 8.5 (\rho_w - \rho_o)(cm) \quad (5)$$

In the three-dimensional model the local density of water is evaluated by the equation of state of sea water. The density of oil can be computed by a table look-up procedure.

In our computation, the local density of sea water associated with the ice formation/salt rejection and advection was evaluated and updated. The results of oil movement beneath the ice under various wind conditions, in the form of response functions computed from the three-dimensional simulation, were recorded on magnetic tape as subsequent inputs to the oil spill trajectory computation.

We found that oil will generally move with ice except under two conditions that cause it to travel at a different speed. The first condition is beneath the shore-fast ice in an area where tidal currents are strong. The second condition is when pack ice is located very close to a passing storm center, when drifting ice abruptly changes direction. Under this condition a high relative velocity between the water and ice can be reached.

Because of the pronounced nonlinear vertical shear coupling, and at high latitude, the direction of an oil movement appears to be extremely variable. Therefore, the vertical shear coupling should be included in the computation even though spilled oil beneath the ice may not seem to be in constant motion with appreciable magnitude.

## MODELING OIL SPILL TRAJECTORIES

Oil spill trajectory computations involve two parts—the first part calculates the movement of oil mainly by advective transport, and the second part calculates the movement of dispersive mechanisms, including weathering, diffusion, and dissolution processes. In this section we will describe the modeling of advective transport only.

Oil transported by advective mechanisms contains several major components. The method used to compute each component is as follows:

**Oil Transport by Mean Wind Drift.** During this computational step, oil movement resulting from wind stress at the surface layer and at different levels in the water column is calculated by the response function technique. The response function represents local advective transient response to a given wind stress. If a three-dimensional model is used to develop these response functions, the effects of transient inertia, bottom, shoreline, and vertical stratification are all included. The computed movement using this response technique gives only the movement near the middle of the surface layer (typically 5 meters) schema-

tized in the 3D model. For the surface movement the results are extrapolated for speed and direction near the surface using an analytical solution of the Ekman type assuming constant density within that surface (mixed) layer.

**Stokes' Transport.** When wind blows over the water surface it generates Stokes' transport in addition to the mean wind-driven current. This transport is caused by the non-linear residual orbital motion associated with the local wind waves field. The magnitude of this transport is a function of the intensity and age of the wave field. The direction is nearly identical to the wave-propagating direction. In the oil spill trajectory model, a special sub-routine is used to compute the direction and speed of this transport. According to measurements in the field and in the laboratory, Stokes' transport is approximately 1.6 percent of the local wind speed if the wave field is not limited by wind duration and fetch length. The wind used to compute the Stokes' transport is obtained from the wind field model described in (Liu and Leendertse, 1987)

**Tidal and Baroclinic Residual Component over the Alaskan Outer Continental Shelf Area.** Because of the complex tidal regime and density field, tidal residual and baroclinic circulation components are quite essential. We have discussed their dynamics in great detail in (Liu and Leendertse, 1987)

To simulate a number of trajectories with the trajectory model, many data are needed from other models that we have previously described. Figure 2 gives an overview of the data flow between these models. As illustrated in the diagram, when computing the oil movement, the oil/trajectory model plays the role of data synthesizer. As physical parameters involved in calculating oil movements are difficult and expensive to measure over the entire Alaskan waters, the model is programmed with flexibility in mind, so that any field data, if available, can be used to drive the model in its simplest mode. On the other hand, the trajectory model would link results from the other models. To perform this task, it contains the basic physical parameters of the entire lease area as well as the grid network of the entire model and submodels within the system.

During the study period, spill trajectory analyses were made on a lease-area basis. For each lease sale, approximately 30 to 40 launch points were selected by the Minerals Management Service according to the potential petroleum resource. The movements of oil were then tracked for a period of time, typically a month during the summer period, to as long as six months during winter.

From each launch location 40 to 60 trajectories are computed under different weather scenarios. For each trajectory, half-hourly positions are computed and landfall locations are recorded where possible. As described above, the wind-driven component of the oil movements is computed using the wind-driven response function technique through the convolution procedure. To maintain accuracy, each response function has half-hourly weighting elements for each wind direction, each computational grid, each layer, and each season. One magnetic tape is required to store all response functions from each of four wind directions. For the computation of oil spill trajectories, this information is transferred to disk storage.

Results from a typical simulation are presented in Fig. 3. In the figure, the computational grid of the three-dimensional model of the Beaufort Sea is superimposed over the oil trajectory model, which also covers the eastern portion of the Chukchi Sea. The response functions and net-current field over that area are averages obtained from the two models.

On top of the graph, computed 12-hour wind vectors sampled at Point Barrow are plotted. The mean winds and half-hourly varying winds from the simulation are also presented in the form of wind roses for speed and direction, also at Point Barrow. The wind direction rose represents the frequency of occurrence of wind direction toward which wind is blowing. A wind speed rose represents the average marine wind speed associated with each of the 16 wind directions mentioned above. The plotting scale of the highest speed in the rose is 12 knots as indicated under the rose.

Each dot in the oil trajectory represents daily displacement originating from the launch point, which is marked by a number. When examining the trajectories one would notice the following interesting aspects:

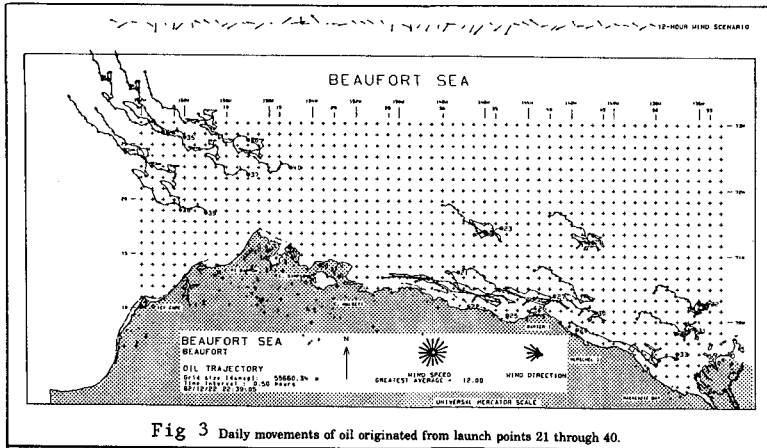


Fig 3 Daily movements of oil originated from launch points 21 through 40.

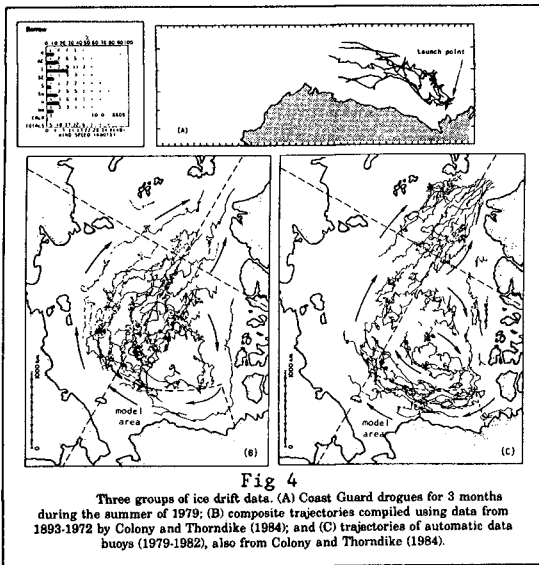


Fig 4

Three groups of ice drift data. (A) Coast Guard drogues for 3 months during the summer of 1979; (B) composite trajectories compiled using data from 1893-1972 by Colony and Thorndike (1984); and (C) trajectories of automatic data buoys (1979-1982), also from Colony and Thorndike (1984).

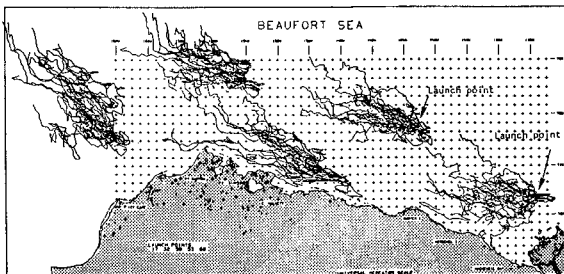


Fig 5 computed by the RAND oil trajectory model and the two-dimensional stochastic weather simulation model.

1. The predominant wind during a summer period is from the east-southeast.
2. Oil spilled closer to the shore travels faster, in a downwind position.
3. Oil spilled offshore moves in a more random direction and has a larger deflection angle. This can be attributed to the greater water depth and the existence of ice floes.
4. Oil spilled further offshore travels in a direction approximately the same as the Arctic Gyre (Colony and Thorndike, 1984, U.S. Coast Guard buoy data, Fig. 4). The simulation in Fig. 4 was made in December 1982.

The trajectories shown in Fig. 3 represent oil movements under a given 30-day weather scenario. In Fig. 5 comparison between satellite-tracked buoys (Murphy et al., 1981) and trajectories computed using the coupled trajectory-weather model is shown. During the summer period, the average observed movement of ice is approximately 140 nautical miles per month. The same is found in the computed monthly average displacement. The observed and the computed trajectory patterns in the Mackenzie Bay are quite irregular. This may be due, in part, to the cyclonic local eddy described above.

Without observed wind fields and the variability of winds, tracing the deterministic motion of a particular ice floe is not as desirable as comparing a group of observed trajectories to a group of computed trajectories using a weather model. The same weather model will be used for the statistical trajectory analyses below.

In the trajectories it can be seen that the impact of a moving storm can sometimes be seen as a loop in a trajectory. The size and shape of the loop vary because of their location relative to the moving storm.

The computed trajectories for the winter season have the similar direction of predominant movement. Figure 6 shows the general direction of movement launched from three selected points. The residence time within the modeled area is approximately two to three months. If all launch points for a given season are considered, one can assess the oil spill risk by counting the number of contact occurrences within each square area whose length is 10 nautical miles in the north-south direction (Fig. 7). In Fig. 7 the size of a circle represents the spatial distribution of landfall frequencies. If oil is trapped in a near-shore lagoon, a continuous contact is assumed for the remaining period. In preparing the map, analysis is made using two-hour counting method. Plotting scale for the circle is 21211, two-hour exposure periods equals one latitudinal grid spacing for the radius of the circle.

If the near-shore entrapments are excluded, a similar diagram (Fig. 8) gives the spatial distribution for the marine resource contact frequencies. In this case, each latitudinal grid spacing equals 1872 two-hour contact period for the radius of a circle. From graphs like Fig. 7 and 8, one would be able to obtain a general assessment of contact risk associated with the oil spill. However, sometimes it is more desirable to estimate the concentration of oil, if a contact is made.

## DETERMINING THE OIL CONCENTRATION FIELD

When released in water, fresh crude oil will undergo major changes in its composition while being transported and dispersed. The spreading of oil at the surface is mainly due to mechanisms associated with viscosity, surface tension, and inertia. As time progresses the major process responsible for the spreading of spilled oil are advection and turbulent dispersion. While oil is being advected and dispersed, its concentration decreases as a result of evaporation, photochemical degradation, and biodegradation. These processes are called weathering.

In modeling an oil concentration field, advection, dispersion, and weathering are considered as well as the transport of oil. The rates of evaporation and the bio- and photochemical degradation were evaluated under field conditions by other investigators (Payne et al., 1983). The oil decay rates for the simulation were estimated by these investigators on the basis of turbulence levels determined by means of the three-dimensional models for the different areas.

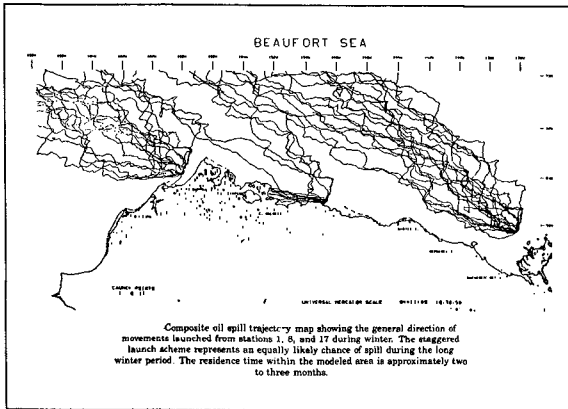


Fig 6

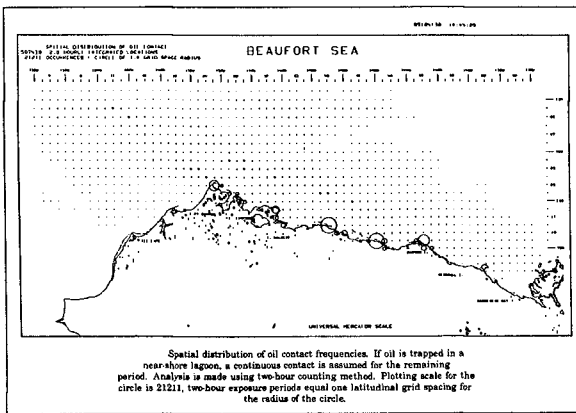


Fig 7

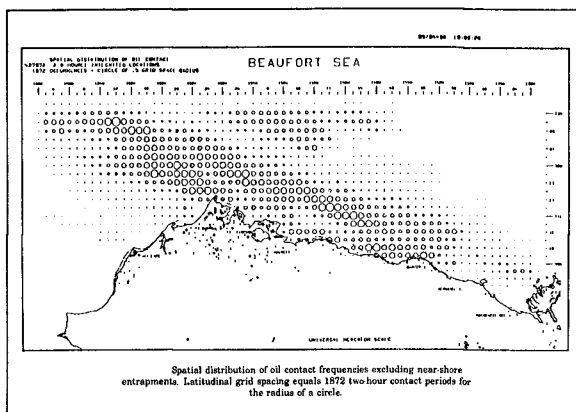


Fig 8

To illustrate the diffusion process induced by the turbulent oscillating flow, it is more convenient to demonstrate the magnitude of diffusion over the vertical plane in the absence of surface energy input from the wind. In other words, in this illustration the turbulence is generated primarily at the bottom by tide. To show the turbulent diffusion processes one hundred particles are released in each vertical layer near the Pribilof Island and half-hourly displacements are plotted there for a period of 24 hours (Fig. 9). The elevations for the eight layers are 2.5, 7.5, 12.5, 17.5, 25, 35, 85, and 240 meters, respectively.

In each layer the movements of particles are caused by advection and diffusion processes. For instance, the hourly displacement of the particle group in the first layer starts from the upper position, gradually moving with the tidal motion. As the group moves the distance between the particles increases because of the turbulent diffusion. In a stricter sense, the separation of particles is the combined result of diffusion and the nonuniformity of the current field. The combined process is called the turbulent dispersion. In shear flow, such as the one illustrated here, the major mechanism responsible for dilution of a soluble is dispersion. This is evident from the amount of dispersion experienced by the particle groups in the lower layers where the velocity gradient is much sharper than in the upper five layers. These five layers are located above the sharp pycnocline, which partially isolates the upward momentum transport.

Also of interest are the distances between the first and the last particle group within each layer. They represent the net displacement over a period of two days. The changes in net transport over the vertical are quite common in the coastal area, to satisfy the law of conservation of mass.

The example presented here illustrates the dispersion mechanism associated primarily with bottom stress and nonuniform velocity distribution. Dispersion effects can also be induced by shore line irregularity through the variability of the velocity field. For each of the large modeled areas, submodels are used to compute near-shore oil movements (Fig. 10). The turbulent diffusion coefficients averaged over ten tidal cycles, as computed by the three-dimensional model for each large area and for each layer, are stored on magnetic tapes. These diffusion coefficients became very useful for diffusion analysis in a limited near-shore area. Figure 11 represents the results of oil dispersion analysis in which crude oil is released instantaneously from five locations near the Bering Strait. Displacement of the one-part-per-billion concentration envelopes are plotted every five days. The influence of the shoreline and the variability of local advective/diffusive mechanisms (Fig. 11) are quite evident, as seen by the changing speed and direction of the oil movement.

Under a scenario of continuous release, the distribution of surface oil concentration is presented in Fig. 11. When oil moves through the Bering Strait, the strong local current tends to elongate the oil. Also notice the cumulation effects when the oil reaches the coastal area, where the on-shore current components drop and the along-shore currents strengthen. This near-shore effect tends to redirect the oil while slowing it down. The speed of an oil transport can be seen from the top diagram of Fig. 12, where daily displacements of the advancing plume are plotted. The daily traveling speed of oil is governed by the evolutionary weather state as well as the local circulation pattern.

To illustrate the effects of weather and local baroclinic circulation, a group of six trajectories are launched from five hypothetical spill locations in the Chukchi Sea/Barrow Arch lease area (Fig. 13). The net displacement for the northern trajectories during the eight-month period ranges between 3–5° latitude, which represents a daily movement of 1.4 to 2.31 km (Fig. 14). Oil launched near Point Hope travels substantially slower than its northern counterpart, which moves predominantly within the Arctic Gyre. The simulated direction and speed of ice movements within the Chukchi Sea agree with the observed values reported by Gordienko (1958), and Hibler (1979), who made computations using ice models including nonlinear plastic flow effects by means of viscous-plastic constitutive law.

Perhaps it is more illustrative to show and analyze a group of trajectories launched near an embayment so that the shore effects can be seen. The launch point is located between St. Lawrence Island and the Gulf of Anadyr, USSR (see the insert map of Fig. 15). Twenty-one



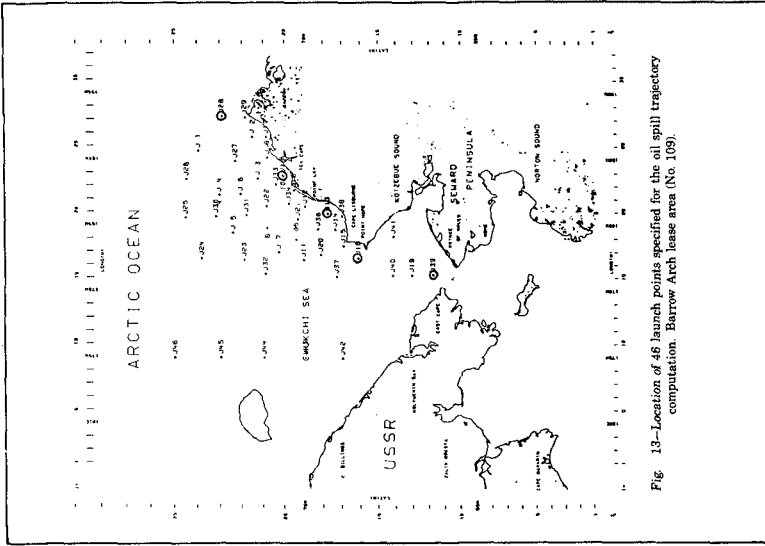


Fig. 13—Location of 46 launch points specified for the oil spill trajectory computation. Barrow Arch. lease area (No. 109).

Fig 13

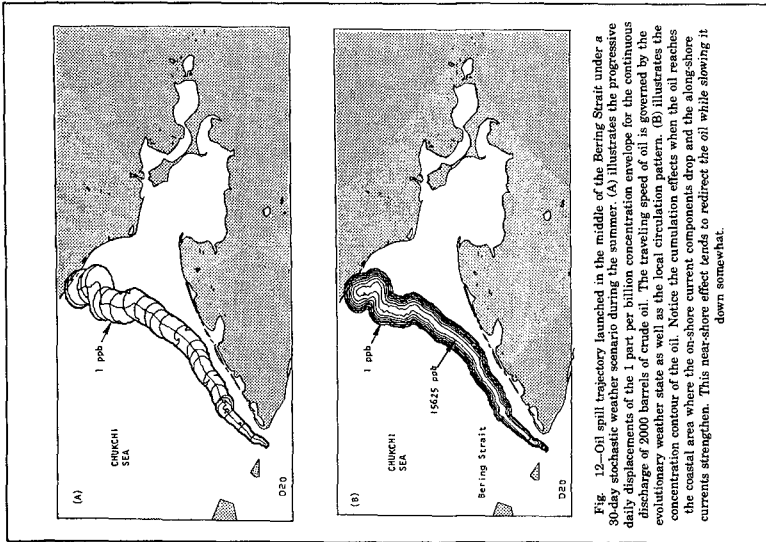


Fig. 12. Oil spill trajectory launched in the middle of the Bering Strait under a 30-day stochastic weather scenario during the summer. (A) illustrates the progressive daily displacements of the 1 part per billion concentration envelope for the continuous discharge of 2000 barrels of crude oil. The traveling speed of oil is governed by the evolutionary weather state as well as the local circulation pattern. (B) illustrates the concentration contour of the oil. Notice the cumulation effects when the oil reaches the coastal area where the on-shore current components drop and the along-shore currents strengthen. This near-shore effect tends to redirect the oil while slowing it down somewhat.

Fig 12

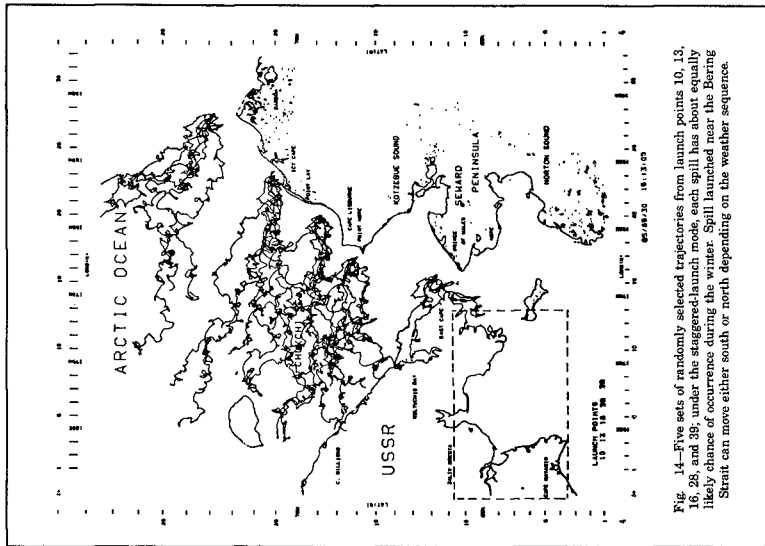


Fig 14

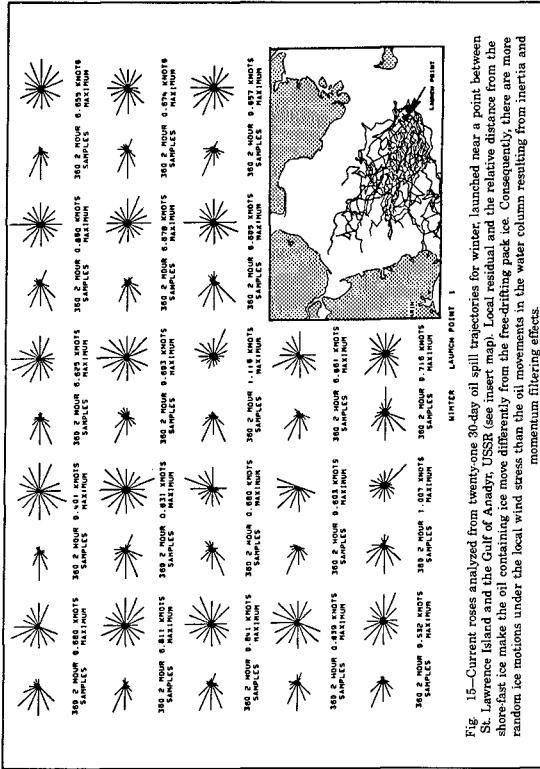


Fig 15



groups of 30-day oil spill trajectories are sampled every two hours. These sampled data are then analyzed for their direction and speed. For a 30-day duration there are 360 two-hour samples for current directions and speeds. Since the directions and speeds of currents at every two hours are located over a different area, local residual circulation and the relative distance from the shore-fast ice make the movement of oil contained in ice different from that of free-drifting pack ice. Consequently, there are more random ice motions under the local wind stress than the oil movements in the water column resulting from inertia and momentum filtering effects.

Figure 16 indicates that most oil spill trajectories move in a predominantly northwesterly direction. For the summer period (Fig. 16), however, most contacts are closer to the eastern shore. It should be noted that the plotting scale of Fig. 17 is four times that of the one shown in Fig. 16. The western Chukchi Sea receives much less impact during the summer season than in the winter period. On the average, oil travels a shorter distance and moves more randomly under the summer winds. During summer, winds have higher variabilities and, as a consequence, the inertial current components have a substantial contribution toward the overall current direction. The area of greatest impact is located near Icy Cape.

#### REFERENCES

- Colony, R., and A. S. Thorndike, (1984): A estimate of the main field of the Arctic ice motion, *J. Geophys. Res.* Vol. 89, No. 6., pp. 10623-10629.
- Cox, J. C., L. A. Shultz, R. P. Johnson and R. A. Sheley, (1980): The transport and behavior of oil spilled in and under sea ice, *Arctic Pac. Rep. No. 460C.*
- Ekman, V. W. (1905): On the influences of the earth's rotation on ocean currents, *Ark. Math. Astr. Fysik. Kong. Su. Vetenskap. Akad., Stockholm*, Vol. 2, No. 11, p. 52.
- Gorgienko, P., (1958): Arctic ice drift, *Proc. Conf. on Arctic sea ice*, Published by the National Academy of Sciences and the National Research Council, Washington, D. C., pp. 210-220.
- Hibler, W. D., (1979): A dynamic thermodynamic sea ice model, *J. Phys. Oceano.* Vol. 9, No. 7., pp. 815-846.
- Kovacs, A., R. M. Morey, and D. Cundy, (1980): Oil pooling under sea ice, *Environmental Assessment of the Alaskan Continental Shelf*, Ann. Rep. Vol. 5, pp. 333-339.
- Liu, S. K., and J. J. Leendertse, (1982): A three-dimensional model of Bering and Chukchi Sea, *COASTAL ENGINEERING* Vol. 18, ASCE, N. Y.
- Liu, S. K., and J. J. Leendertse, (1984): A three-dimensional model of Beaufort Sea, *COASTAL ENGINEERING* Vol. 19, ASCE, N. Y.
- Liu, S. K., and J. J. Leendertse, (1986): A three dimensional model of the Gulf of Alaska, *COASTAL ENGINEERING* Vol. 20, ASCE, N. Y.
- Liu, S. K., and J. J. Leendertse, (1987): Modeling the Alaskan Continental Shelf Waters, *RAND R-3567-NOAA/RC*, 136 pages.
- Murphy, D. L., P. A. Tebeau, and L. M. Lissner, (1981): Long-term movements of satellite-tracked buoys in the Beaufort Sea, Office of Research and Development, U. S. Department of Transportation, CG-D-48-82.